Aquat Geochem (2014) 20:39–57
DOI 10.1007/s10498-013-9206-7

ORIGINAL PAPER

Submicromolar Oxygen Profiles at the Oxic–Anoxic Boundary of Temperate Lakes

Mathias K. Kirf · Christian Dinkel · Carsten J. Schubert · Bernhard Wehrli

Received: 13 June 2013 / Accepted: 12 September 2013 / Published online: 17 October 2013
© Springer Science+Business Media Dordrecht 2013

Abstract Elements involved in biogeochemical cycles undergo rapid turnover at the oxic–anoxic interface of stratified lakes. Here, the presence or absence of oxygen governs abiotic and biotic processes and rates. However, achieving a detailed sampling resolution to precisely locate the oxic–anoxic interface is difficult due to a lack of fast, drift-free sensors in the working range of 10 to a few 1,000 nmol O_2 L^{-1}. Here, we demonstrate that conventional amperometric and optical microsensors can be used to resolve submicromolar oxygen concentrations in a continuous profiling mode. The amperometric drift was drastically reduced by anoxic preconditioning. In situ offset correction in the anoxic layer and a high amplification scheme allowed for an excellent detection limit of < 10 nmol L^{-1}. The optical microsensors also showed a similar performance with a detection limit of < 20 nmol L^{-1}. Their drift stability allowed for a laboratory calibration in combination with a minor in situ anoxic offset correction. The two different sensor systems showed virtually identical profiles during parallel use in stratified lakes. Both sensors were able to resolve the fine-scale structure at the oxic–anoxic interface and revealed hitherto unnoticed extended zones of submicromolar oxygen concentrations even below a steep oxycline. The zones extended up to several meters and showed substantial vertical variability. These results underline the need of a precise localization of the oxic–anoxic interface on a submicromolar scale in order to constrain the relevant aerobic and anaerobic redox processes.

Keywords Oxic–anoxic interface · Nanomolar oxygen · Detection limit · Anoxia · Redox · Gradient · Stratification · Optode · Amperometric · Microsensor · Signal drift

M. K. Kirf (✉) · C. Dinkel · C. J. Schubert · B. Wehrli
Department of Surface Waters - Research and Management, Eawag, Swiss Federal Institute of Aquatic Science and Technology, 6047 Kastanienbaum, Switzerland
e-mail: mathias@kirf.de

M. K. Kirf · B. Wehrli
Institute of Biogeochemistry and Pollutant Dynamics, ETH Zurich, 8092 Zurich, Switzerland

1 Introduction

One of the main questions in analytical biogeochemistry is whether oxygen is present or not in any given aquatic environment (Berner 1981; Canfield and Thamdrup 2009). Of particular significance for redox-cycling is hence the oxic–anoxic interface. Most of the redox processes at the oxic–anoxic interface are mediated by microorganisms which are either dependent on or inhibited by oxygen. Detecting oxygen at very low concentrations is therefore of utmost importance to precisely locate the oxic–anoxic interface (Wright et al. 2012; Thamdrup et al. 2012).

Traditionally, anoxic waters are defined by the lowest oxygen concentration measurable by standard techniques, such as the Winkler method (Winkler 1888), with the accepted limit being set to $\sim$1 μmol L^{-1} (Berner 1981; Morrison et al. 1999; Canfield and Thamdrup 2009). Only with the recent introduction of the Switchable Trace OXygen (STOX)-sensor was this limit pushed to below 10 nmol L^{-1} (Revsbech et al. 2009). The STOX-sensor provided new insights into oxygen and nutrient dynamics within the extensive marine oxygen minimum zones (Kalvelage et al. 2011; Thamdrup et al. 2012; Ulloa et al. 2012) such as the recent observation of extremely low half saturation constants below 150 nmol L^{-1} for aerobic respiration and growth (Revsbech et al. 2009; Stolper et al. 2010). These studies demonstrated that the traditional detection limit of 1 μmol O_2 L^{-1} was at least one order of magnitude above the sensitivity needed to fully investigate when and how oxygen depletion terminates aerobic life and changes redox pathways that couple the anoxic with the oxic part of aquatic systems (Kalvelage et al. 2011; Lam et al. 2009; Ulloa et al. 2012). Furthermore, reliable low concentration O_2 measurements would allow to target sampling locations for microbial communities thriving at the oxic–anoxic transition such like nitrifiers, denitrifiers, anammox bacteria or aerobic methane oxidizers (Kalvelage et al. 2011; Schubert et al. 2006; Lopes et al. 2011).

Currently, we know little about the extensions, the variability and the biogeochemical significance of zones with submicromolar oxygen concentrations. In many aquatic systems, the oxic–anoxic transition is dynamic and the associated reactions occur on relatively small spatial scales (Murray et al. 1995; Lopes et al. 2011). Achieving a detailed sampling resolution and a precise localization of the oxic–anoxic interface in the water column is hence not possible due to a lack in drift-free and fast sensors in the working range of 10 to a few 1,000 nmol O_2 L^{-1}.

Useful profiling and sampling systems for the lower limit of the oxic zone require high sensitivity down to the nanomolar range. They should provide a continuous, fast responding signal to give reasonable spatial resolution and a clean, ideally drift-free zero oxygen signal. Clark-type amperometric oxygen microsensors with a guard cathode (Revsbech 1989; Clark et al. 1953) do meet most of these requirements. Their output can be amplified and registered continuously with very high sensitivity. These sensors show excellent 90 %-response times down to 0.2 s (Berg et al. 2003), and the linear relationship between the signal and oxygen partial pressure is well documented (Revsbech and Jørgensen 1986; Reimers 1987; Revsbech 1989). The temperature dependency of the signal and its stirring-sensitivity are tractable problems, but the drift at low oxygen concentrations has so far limited the practical detection limit to about 1 μmol L^{-1} (Reimers 1987; Revsbech et al. 2011). Zero-signal stability might further deteriorate at euxinic conditions due to the H_2S-sensitivity of these sensors; however, such depths are avoidable in many aquatic systems.

The Clark-type amperometric STOX-sensor avoids the drift problem by introducing a secondary (front) cathode that can be polarized in order to prevent oxygen from reaching

the internal sensing cathode, thus providing in situ zero calibration (Revsbech et al. 2009). With its differential measurement, the sensor reaches detection limits in the nanomolar range. This advantage, however, comes at the cost of long measuring intervals of typical 1–4 min per measurement cycle, which limits the continuous profiling capabilities of this system.

Optical oxygen microsensors with highly oxygen-sensitive fluorescent coatings, hereafter referred to as microoptodes, offer a further possibility to trace low oxygen concentrations (Klimant et al. 1995; Holst et al. 2000; Nestler et al. 2007). Their signal-to-noise ratio at submicromolar oxygen concentrations is excellent as the fluorescence intensity and fluorescence lifetime increase with decreasing oxygen partial pressure. The temperature-sensitivity of optodes can be corrected for, minimal signal drift is realized by a lifetime-based measuring technique, and in addition, they show no sensitivity to stirring rates or H_2S (Lippitsch et al. 1988; Tengberg et al. 2006). Excellent low detection limits of 30–60 nmol O_2 L^{-1} have been reported for optodes with highly oxygen-sensitive fluorescent coatings (Nestler et al. 2007; Balcke et al. 2008), and they offer the potential to investigate the oxic–anoxic boundary in more detail.

In the present study, we adapted two different in situ oxygen-sensing technics to explore the submicromolar oxygen distribution at the oxic–anoxic boundaries in lakes. As a tool for such investigations, we developed the "Profiling In situ Analyzer" (PIA), an online-controlled measurement and sampling platform that allows resolution of the fine-scale structure of the oxic–anoxic interface by continuous profiling down to nanomolar oxygen levels and enables targeted sampling.

The system allows for cross-check and validation by two independent sensor systems by combining amperometric microsensors with microoptodes. Utilizing the anoxic water layer for preconditioning of the amperometric sensors and as an in situ calibration point drastically improved the amperometric sensor performance at low oxygen conditions, solving issues of drift and zero oxygen signal offset associated with these sensors. The detection limits, signal stabilities and reproducibilities between the two systems were tested in the field. The system was then applied for profiling the oxic–anoxic boundary in two Swiss lakes to characterize the extension and variability of the submicromolar oxygen zone. With their broad range of redox conditions and good accessibility, lakes constitute an ideal laboratory for the assessment of oxygen-sensing technology and to further investigate the concepts of biogeochemical zonation (Tonolla et al. 2004; Lopes et al. 2011; Canfield and Thamdrup 2009).

2 Materials and Methods

2.1 Profiling In Situ Analyzer (PIA)

In situ measurements were performed with a custom-built profiling analyzer, which was designed for flexible online data acquisition, analysis and visualization based on embedded computing (ZBrain, Schmid Engineering, Switzerland). Instruments are mounted in front of an open cubic aluminum frame of 50 × 50 × 60 cm which holds on its top the processing unit and its power supply in pressure stable housing and leaves room in the center for a carousel syringe sampler with 12 × 60 ml syringes (KC Denmark, Denmark) (Fig. 1a). Two-way communication along a galvanically isolated load-carrying data cable allows online evaluation of depth profiles on shipboard via a laptop computer and thus targeted sampling. The device was deployed by an electric winch. Customized software for

embedded computing and data acquisition was written with LabVIEW (National Instruments, USA). Data were further processed with custom MATLAB scripts (The MathWorks, USA). Oxygen concentrations were measured with two different O_2 sensor systems optimized for low oxygen concentrations as described below.

2.2 Amperometric Oxygen Microsensor

Measurements were performed with Clark-type amperometric microsensors with a tip diameter of 25 µm and equipped with an internal reference and a back guard as introduced by Revsbech (1989) (Ox-25, typical 90 %-response time <0.5 s, Unisense, Denmark). Compared to conventional oxygen microelectrodes, drift at low oxygen concentration was strongly reduced by a preconditioning procedure which presumably lowered dissolved oxygen concentrations in the bulk electrolyte of the sensors: 36 h prior to deployment, the sensor was exposed to anoxic conditions by fitting a closed-bottom plastic tube around the sensor filled with anoxic solution (0.1 mol L^{-1} sodium ascorbate mixed with 0.1 mol L^{-1} sodium hydroxide, solution prepared from degassed water). After removal of the tube in the field, fast descent of the profiler through the oxic water column limited accumulation of dissolved oxygen in the microsensor. To further reduce signal drift, the microsensor was operated for 1–4 h in the anoxic water column and subsequent upcasts during profiling were limited to low oxic conditions. The amperometric signal at low oxygen concentrations was amplified with factors of up to 20,000 to increase the digital resolution in this concentration range (Fig. 1b). High amplification factors were only applicable under submersed in situ conditions due to the prevalent electromagnetic noise in most laboratories. Higher oxygen concentrations were recorded with lower amplification on parallel channels.

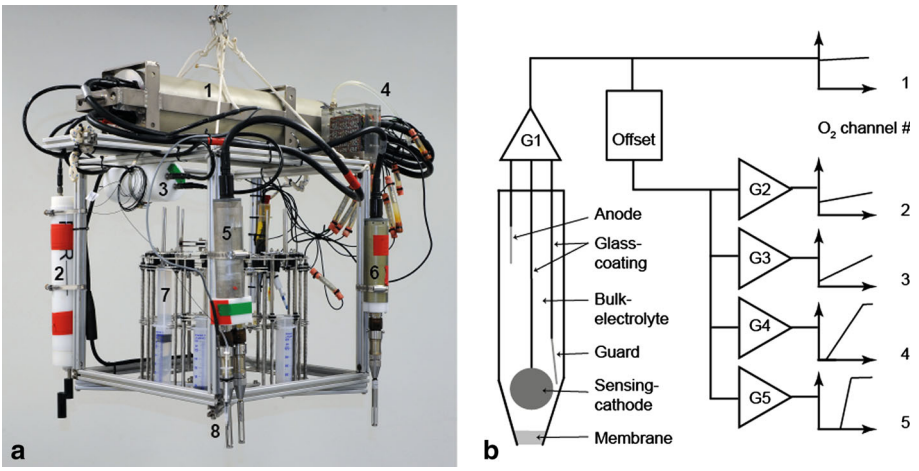

Fig. 1 **a** Typical setup of the Profiling In situ Analyzer (PIA): *1* Pressure housing (embedded computer, electronics, batteries), *2* CTD probe, *3* optode module, *4* impedance converter for potentiometric channels (pH, Redox, S^{2-}), *5* oxygen preamplifier, 6 sulfide preamplifier and amperometric sulfide microsensor, *7* syringe sampler, *8* oxygen sensor array: microoptode (syringe), up to two amperometric microsensors. **b** Signal-pathway of the amperometric setup. *G1* Preamplifier, *G2–G5* second amplification stage, *Offset* offset correction of the zero oxygen signal to match the input range of the A/D converter

2.3 Signal-Pathway

The microsensor was connected by an in situ connector system (Unisense, Denmark) to a custom-built preamplifier. Here, the current signal of the microsensor was converted into a voltage signal (1 mV pA^{-1}, OPA 128, Burr-Brown, USA) and amplified 10 times (AD524, Analog Devices, USA). The voltage signal was passed through a low-pass fourth-order Bessel filter to attenuate electromagnetic noise above 15 Hz in the laboratory and after that through a galvanic isolation which prevented ground loops (ISO124, Burr-Brown, USA). The preamplifier was connected with an underwater cable and connectors (SubConn Circular, SubConn, USA) to the PIA's processing unit in pressure stable housing where the signal was transmitted to two channels. The first channel with overall gain of 10 passed directly to a multiplexer, and readings were taken by a 14-bit A/D converter (Fig. 1b). A single reading consisted of 10 samples taken at 500 Hz, which were averaged and stored at 2 Hz. This channel captures the whole range of oxygen concentrations from 0 to air saturation. The second channel passed through an offset correction where the zero oxygen signal could be adjusted online to the input range of the A/D converter before being transmitted to 4 channels which were amplified to overall gains of 100, 1,000, 4,681 and 20,000. These four channels passed a multiplexer, and their individual readings were taken consecutively every 0.125 s as described above and stored at 2 Hz. The overall 90 %-response time of the sensing system was 9 s as determined by moving the sensors rapidly from air into stirred anoxic solution.

2.4 Oxygen Microoptode

Measurements were performed with needle-type microoptodes coated with dyes optimized for trace oxygen concentrations (TOS7-dye, 140 µm tip diameter, white optical isolation, PreSens, Germany), with a 90 %-response time of 7 s (determined as described above). During dual sensor profiling, the sensor tips of both systems were mounted at the same height and 1 cm apart. The microoptode was connected by a custom-made optical underwater connector to a phase detection board for luminescence lifetime detection based on phase modulation (O_2-micro-T4D, PreSens, Germany) placed in a pressure stable housing. The raw data output provided at 1 Hz (° phase shift, amplitude, temperature) was transferred via RS-232 interface and logged in the processing unit. A malfunctioning of the optical unit of the board resulted in strong noise in the microoptode data during the Lake Lugano campaign in 2009 and prohibited a quantitative evaluation of the microoptode data. After exchange of the optical unit, the noise was greatly reduced.

2.5 Derived Units and Oxygen Solubility $C^*_{O_2}$

Pressure, conductivity and temperature were recorded by a CTD probe (XR-420, RBR, Canada) with a sampling rate of 2 Hz and logged in the processing unit. Depth was calculated using a density of water of 1 kg L^{-1}. Density profiles were computed by expressing any changes in specific conductivity as changes in the calcium–carbonate concentrations (Imboden and Wüest 1995).

Both types of sensors respond to the partial pressure of oxygen. The oxygen partial pressure in water was related to oxygen concentrations C_{O_2} in µmol L^{-1} by the computed oxygen solubility $C^*_{O_2}$ at standard air pressure p^* (101,325 Pa). $C^*_{O_2}$ was computed as a function of salinity and temperature according to Garcia and Gordon (1992) using the

solubility coefficients derived from the data of Benson and Krause (1984). We use the concentration scale here because it is independent of temperature and pressure, and it facilitates mass balance calculations and modeling. For the biological response to low oxygen conditions, the relevant parameter is partial pressure (Hofmann et al. 2011).

2.6 Calibration of the Microoptodes

In 2009, the microoptode was used only qualitatively due to a malfunction of the optical board. In 2010, the microoptode was calibrated in the laboratory in nanopure water equilibrated with certified gas mixtures according to:

$$\frac{C_{\mathrm{o_2}}}{C^*_{\mathrm{o_2}}} = \frac{C_{\mathrm{o_2\ gas}}}{C_{\mathrm{o_2\ air}}} \times \frac{p_{\mathrm{atm.}}}{p^*} \tag{1}$$

where $C_{\mathrm{o_2}}/C^*_{\mathrm{o_2}}$ denotes the air saturation computed at standard pressure p^*, $C_{\mathrm{o_2\ gas}}$ the specified volume fraction of oxygen in the gas mixture and $C_{\mathrm{o_2\ air}}$ the assumed average volume fraction of oxygen in air of 20.9 % corrected for the deviation of the atmospheric pressure during calibration $p_{\mathrm{atm.}}$ from p^*.

A 1-L Erlenmeyer flask was filled to its neck with nanopure water and cooled to 1–2 °C in ice water. The oxygen content of the water was modified with either nitrogen gas (purity: 99.999 %) or a certified 1.5900 % oxygen in nitrogen gas mixture (PanGas, Switzerland) by low gas-flow dispersed through Tygon-tubing and an aquarium diffuser 10 cm below water level. The water volume was well mixed by a glass-coated magnetic stirrer, and the temperature was monitored by a PT 100-sensor connected to the microoptode-board. A 3-cm-thick, loosely compressed wad-plug placed 4 cm above the water level ensured a defined gas-filled, pressure-equilibrated headspace. Atmospheric pressure was recorded with the CTD pressure sensor. The microoptode was placed opposite to the gas-inflow and calibration values for 0 % and the computed air saturation was only accepted when the signal was constant for at least 6 min.

In contrast to amperometric microsensors, the microoptodes show a nonlinear decrease in fluorescence lifetime with increasing oxygen concentration (Holst et al. 1995). For oxygen concentrations below 35 µmol L^{-1}, the signal of the fluorescent dye type TOS7 follows the Stern–Volmer equation:

$$\frac{\tau_0}{\tau} = \frac{\tan\phi_0}{\tan\phi} = 1 + K_{\mathrm{SV}} \times \frac{C_{\mathrm{o_2}}}{C^*_{\mathrm{o_2}}} \tag{2}$$

where τ_0 and τ are the fluorescence lifetimes, φ_0 and φ are the phase angles in the absence and presence of oxygen, respectively, and K_{SV} is the Stern–Volmer quenching coefficient (Lippitsch et al. 1988; Holst et al. 1995). Temperature affects the fluorescence lifetime and the quenching efficiency of the microoptode (Holst et al. 2000). The temperature dependency of φ and K_{SV} were taken into account by a second-order polynomial:

$$a_{i,\ T_\beta} = a_{i,\ T_\alpha} + b_i\left(T_\alpha - T_\beta\right) + c_i\left(T_\alpha^2 - T_\beta^2\right) \tag{3}$$

where a_i denotes either φ_0 or K_{SV}, b and c are the respective dye-specific coefficients provided by the manufacturer and T_α and T_β are the temperatures during the calibration and the measurement, respectively. K_{SV} values at 4 °C calculated from the manufacturers calibration sheet at 4.7 % air saturation at standard pressure p^* agreed with our laboratory-calibration-derived values for the two applied optodes within 3.4 %.

Below the oxic–anoxic interface, the stabilized in situ zero readings of the microoptode were averaged over ~25 cm and subtracted as offset from the laboratory-calibration-derived oxygen values (Fig. 2c).

2.7 In Situ Calibration of the Amperometric Microsensors

Linear two-point calibrations were performed in situ using an oxic and an anoxic reading (Fig. 2a, b). Anoxic readings were obtained by averaging the zero current over ~25 cm directly after signal stabilization in the (anoxic) water column.

In 2010, a lower amplified O_2-channel of the amperometric microsensor was anchored in each profile on a single microoptode-derived in situ concentration in the range of 6–18 µmol O_2 L^{-1} at depths with weak or nearly absent oxygen gradients. The slope obtained for this lower amplified channel was then used to calculate the slopes of the remaining channels based on the fixed amplification factors. All channels were individually offset-corrected in the anoxic water column. The larger dynamic range of the amperometric microsensor system compared to the microoptode allowed then for an additional validation of the amperometric calibration at higher concentrations of >200 µmol O_2 L^{-1} with a Winkler-calibrated CTD sensor (CTD60M, Sea & Sun Technology, Germany). The correspondence was typically in the range of 2.5 % (data not shown).

During the Lake Lugano campaign in 2009, the optode allowed only for qualitative measurements and the oxic reading was taken on the first O_2 channel at 60 m on the final upcast and was set equal to oxygen concentrations derived from water samples taken at 60 m with a Niskin-bottle and analyzed by Winkler titration. The calculated slopes were then applied to the downcasts with no available oxic reading. All channels were offset-corrected with a one-point calibration in anoxic waters. This approach relies on the

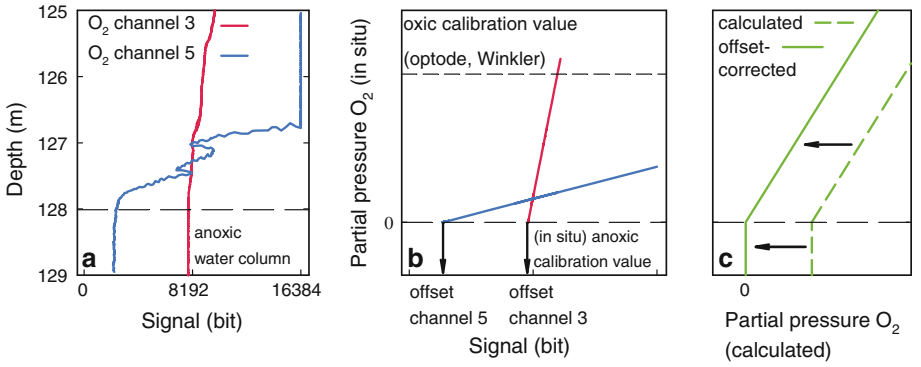

Fig. 2 Schematic example of the in situ calibration procedures for the amperometric sensor (**a**, **b**) and the microoptode (**c**). **a** Lake Lugano: Example of raw signals from two oxygen channels differing in amplification. *Note* The constant signal of O_2 channel 5 on the right is set by the limited input range of the A/D converter. **b** Scheme illustrating how the oxic reading for a lower amplified O_2 channel is matched to microoptode-derived oxygen concentrations between 6 and 18 µmol L^{-1} (e.g., channel 3, 2010) or Winkler-titrated water samples with concentrations above 150 µmol O_2 L^{-1} (channel 1, 2009). Anoxic values are individually obtained in the anoxic water column. Slopes for channels without oxic readings are calculated based on the fixed amplification factors. (**c**) Scheme illustrating how the microoptode's anoxic reading calculated as partial pressure based on the ex situ calibration in the laboratory is applied as offset to all microoptode-derived values

inherent stability of the dynamic part of the signal from Clark-type microsensors (Reimers 1987; Gundersen et al. 1998).

The response of amperometric microsensors is sensitive to stirring rates, changes in temperature ($\approx$2–3 % per °C) and pressure (≈ -0.004 % per meter water column) (Reimers 1987; Gundersen et al. 1998). However, the motion during continuous profiling deployment suggests full sensor response with respect to stirring rates (Revsbech et al. 2011). Temperature gradients below the thermocline were on the order of ± 0.002 °C m^{-1} in Lake Zug and Lake Lugano, and depths between calibration points were less than 100 m. Thus, the temperature and pressure dependencies were negligible, and no corrections were applied. In Lake Rot, the amperometric oxygen sensor was used below the thermocline only qualitatively to confirm features in the microoptode data.

2.8 Onset of H_2S

In Lake Lugano, the onset of the sulfidic zone was determined qualitatively with an amperometric sulfide microsensor (H_2S-100, Unisense, Denmark, specified detection limit: 0.3 µmol L^{-1}). Resolution at low concentrations was increased by parallel amplification on 3 channels in a similar way as described for the oxygen electrodes above. For lakes Zug and Rot, water samples were collected with the syringe sampler on selected casts, 2 ml preserved with 1 ml of 4 % Zn acetate in 2 % acetic acid and kept dark at 4 °C until photometric analysis in the laboratory according to Cline (1969) with a 10-mm cuvette at 670 nm (detection limit 2 µmol L^{-1}, Hitachi U-2000, USA). No H_2S was detected in the profiled water column of Lake Zug. In Lake Rot, an onset of H_2S was detected $\sim$30 cm below the oxic–anoxic interface during cast Rot1 (Fig. 3).

2.9 Sampling Procedure

The position of the oxic–anoxic interface was monitored online based on the microoptode data. To reduce the risk of sampling artefacts like self-induced mixing, we retrieved the profiler very slowly from its anoxic position used for signal stabilization. The boat was then moved by a few meters before a new profile was recorded at slow dive speeds of 0.7 to 2.9 m min^{-1} (Table 1). All three lakes provided excellent conditions for boat-based

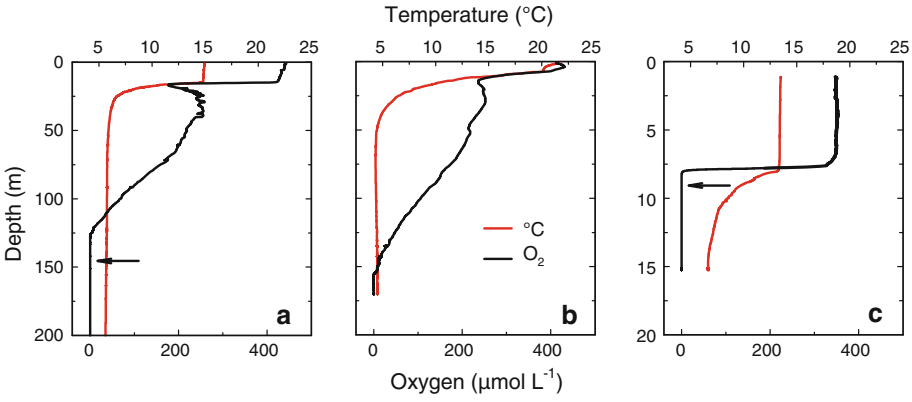

Fig. 3 Oxygen and temperature profiles of Lake Lugano (**a**), Lake Zug (**b**) and Lake Rot (**c**). The *arrows* indicate the onset of H_2S; in Lake Zug no H_2S was found in the profiled water column

Table 1 Characteristics of the individual casts taken in Lake Lugano, Lake Zug and Lake Rot

Cast	Figure	Extension of submicromolar zone (1,000–10 nmol O_2 L^{-1}) (m)	Water depth of oxic–anoxic interface (10 nmol O_2 L^{-1}) (m)	Dive speed (m min^{-1})
Location and date of sampling: Lake Lugano, September 27, 2009				
Lug1	3a, 4a	–	~128	2.0
Lug2		1.3	128.2	0.7
Lug3	4b	1.5	128.0	1.1
Lug4		1.9	125.6	1.6
Location and date of sampling: Lake Zug, August 7, 2010				
Zug1		2.5	161.8	1.7
Zug2		1.6	161.6	1.0
Zug3		1.7	161.0	2.3
Zug4	5a, b	2.5	158.5	2.4
Zug5	5c, d	0.6	156.1	1.8
Zug6	5e, f	3.0	154.9	1.4
Zug7	5g, h	5.6	158.6	2.5
Zug8		4.3	158.2	2.9
Zug9	5i, j	2.5	157.5	2.3
Location and date of sampling: Lake Rot, October 19, 2010				
Rot1	6a, b	0.7	8.7	0.9
Rot2	6a, b	0.2	8.6	0.7
Rot3	6c, d	2.5	10.6	0.8
Rot4	6c, d	0.2	8.5	0.7
Rot5	6c, d	1.3	9.4	0.7

profiling and sampling with wind-shielded, calm and nearly smooth water surfaces during sampling.

2.10 Study Sites

Lake Lugano (46.01°N, 9.02°E) on the border between Switzerland and Italy is separated into two basins by a dam. Measurements were performed close to Gandria in the northern basin which is shielded from winds by steep mountains. The basin has a maximum depth of 288 m, a surface area of 27.5 km^2, a volume of 4.69 km^3 and a mean hydraulic residence time of 12.3 years (Barbieri and Polli 1992). In October 2009, the oxic–anoxic interface was found at ~125 m in the weakly stratified hypolimnion ($\Delta T < -0.001$ °C m^{-1}, $\Delta\kappa_{25} < 0.1$ µS cm^{-1} m^{-1}) (Fig. 3a).

Lake Zug (47.10°N, 8.48°E) in central Switzerland has a maximum depth of 198 m, a surface area of 38.3 km^2, a volume of 3.2 km^3 and a mean hydraulic residence time of ~14 years (Maerki et al. 2009). Measurements were performed in the deep south basin which is shielded from westerly winds by high mountains and not influenced by the main inflow. The south basin remains permanently anoxic below 160 m despite a weakly stratified hypolimnion ($\Delta T < 0.002$ °C m^{-1}, $\Delta\kappa_{25} < 0.1$ µS cm^{-1} m^{-1}) (Fig. 3b).

Lake Rot (47.07°N, 8.32°E) is a dimictic eutrophic prealpine lake close to the city of Lucerne, Switzerland. Lake Rot has a maximum depth of 16 m, a surface area of 0.46 km^2, a volume of 0.0039 km^3 and a mean hydraulic residence time of 0.4 years (Kohler et al.

1984). Measurements were performed in the deepest part of the lake. Lake Rot is shielded from winds by low hills, and a stable stratification ($\Delta T \sim -2$ °C m^{-1}, $\Delta\kappa_{25} \sim 10$ μS cm^{-1} m^{-1}) establishes between May and November with a strong chemocline (8–11 m) and an anoxic, sulfidic hypolimnion (Fig. 3c).

3 Results and Discussion

We used the PIA-system for continuous profiling down to nanomolar concentrations and across the oxic–anoxic interface in the water column of three aquatic environments: (1) The stabilization of amperometric signal drift was assessed in Lake Lugano; (2) in Lake Zug, the absence of significant temperature gradients and the absence of H_2S in the deep hypolimnion allowed cross-validation of amperometric microsensor and microoptode results by simultaneous profiling with the two independent systems; (3) in the temperature-stratified Lake Rot, the performance of the microoptode below a steep oxycline and across a temperature gradient was investigated. The contrasting field sites allowed exploration of the extent and variability of the submicromolar oxygen zone in a deep hypolimnion and at a thermocline.

3.1 Stabilizing Amperometric Drift

The effect of anoxic preconditioning on the reduction in amperometric signal drift at low oxygen concentrations was assessed during a campaign in Lake Lugano. Direct profiling from the lake's surface with an oxygen exposure of 21 min (Fig. 4a) caused the signal of the amperometric microsensor to drift −560 nmol L^{-1} min^{-1} when reaching anoxic waters. The subsequent profiles were obtained after 133 and 140 min of anoxic conditioning at 130–140 m depth (one profile shown in Fig. 4b). This procedure reduced signal drift within the first minute in anoxic waters to <0.5 % of the initial drift, e.g., to −2.1 and −1.5 nmol L^{-1} min^{-1}, respectively, and allowed the localization of the oxic–anoxic interface. Within the next 4 min at anoxic conditions, drift was further reduced to −0.4 and −1.2 nmol L^{-1} min^{-1}, respectively. The in situ detection limit (calculated as two times the standard deviation of the anoxic signal) of the amperometric microsensor for the two downcasts was 4.5 ± 0.7 nmol L^{-1}. The theoretical digital resolution was two orders of magnitude better (0.06 nmol bit^{-1}). The oxygen microsensor showed excellent stability in the anoxic water column until H_2S appeared about 16 m below the oxic–anoxic interface (arrow in Fig. 4b). However, electromagnetic noise, e.g., caused by the activation of the syringe sampler, will propagate as strong peaks into the highly amplified amperometric signal which impedes exact measurements during sampling (data not shown).

The preconditioning approach presented here was inspired by the observation that signal drift in anoxic waters was correlated with previous exposure to oxic conditions. Back diffusion of oxygen from the bulk electrolyte to the sensing cathode in spite of the polarized guard cathode could explain the observed drift after oxic exposure (Fig. 1b). The guard cathode contributes significantly to amperometric signal stability at low oxygen concentrations by consuming such back-diffusing oxygen (Revsbech 1989). However, a non-quantitative consumption of oxygen by a (front) guard cathode was described recently for the STOX-sensor (Revsbech et al. 2009). Apparently, preconditioning the amperometric microsensor under anoxic conditions stabilized the signal at trace oxygen conditions. Therefore, the anoxic pre-deployment and the limited exposure to elevated oxygen concentrations during profiling might have eliminated oxygen in the bulk electrolyte and

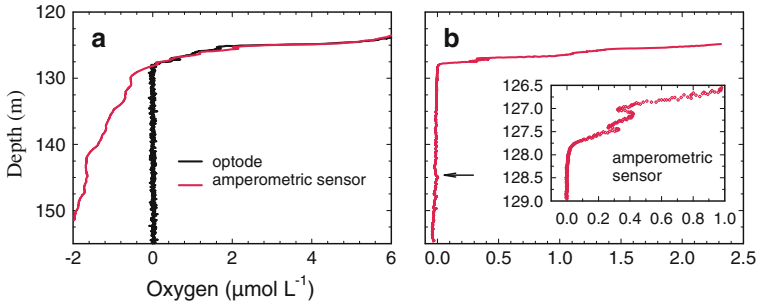

Fig. 4 Lake Lugano, October 27, 2009: Signal drift before (**a**, 10 m ≈5 min) and after (**b**, 10 m ≈9 min) ~2 h of anoxic incubation of the amperometric microsensor. Optode in **a** indicates the depth of the oxic–anoxic interface which was used for anoxic calibration. Negative O_2-values of the amperometric microsensor are caused by drift. *Arrow* in **b**: The H_2S-microsensor indicates the onset of H_2S at 144.5 m, and at this depth, the O_2-signal destabilized again

reduced any resupply of oxygen via the tip, thus eventually reducing drift. Submicromolar oxygen concentrations were well resolved with the high amplification scheme, and the setup achieved a detection limit below 5 nmol L^{-1} at a significantly reduced drift (< -1.5 nmol L^{-1} min^{-1}) with commercial amperometric microsensors. In contrast to the STOX-sensor, this conditioning approach allows for continuous profiling across the oxic–anoxic interface, but it requires a completely anoxic, preferably H_2S-free part of the water column and several hours of pre-deployment.

3.2 Microoptode and Dual Profiling

In the deep hypolimnion of weakly stratified Lake Zug, the microoptode and the amperometric microsensor were evaluated in parallel in the absence of H_2S and significant temperature gradients. The data acquisition for the microoptode was optimized after the first trial in Lake Lugano. During the Lake Zug campaign, the microoptode resolved submicromolar oxygen concentrations with an in situ detection limit of 12.9 ± 1.1 nmol L^{-1} ($n = 6$) with a digital resolution of 4 nmol L^{-1} per 0.01° increment in phase shift and with no detectable drift in the anoxic zone. The ex situ calibration always showed a positive offset at anoxic in situ conditions, although with a maximum deviation of < 24 nmol L^{-1} (see Fig. 2c).

The amperometric in situ detection limit was 10.6 ± 2.2 nmol L^{-1} ($n = 5$), and the dual sensor setup which acquired two submicromolar profiles in parallel (Fig. 5) allowed the cross-checking of the microoptode against the amperometric microsensor. The correlation coefficient between amperometric and optical data in Fig. 5 is at least 0.995. The excellent match of profiles in the submicromolar oxygen range obtained by two completely different analysis techniques is encouraging and indicates that the observed patterns are caused by actual concentrations gradients and not by problems of the sensing systems and their measuring principle. Furthermore, the signals of the two independent systems stabilized at their anoxic reading at similar depths, indicating that the oxygen partial pressure dropped simultaneously below the sensitivity of both systems (Fig. 5). The sensitivity of Clark-type amperometric microsensors down to nanomolar concentrations has been demonstrated by ex situ experiments before (Revsbech et al. 2009). We conclude that at given in situ conditions both systems are sensitive down to nanomolar oxygen concentrations. The long-term drift stability of the microoptode allowed for laboratory calibration

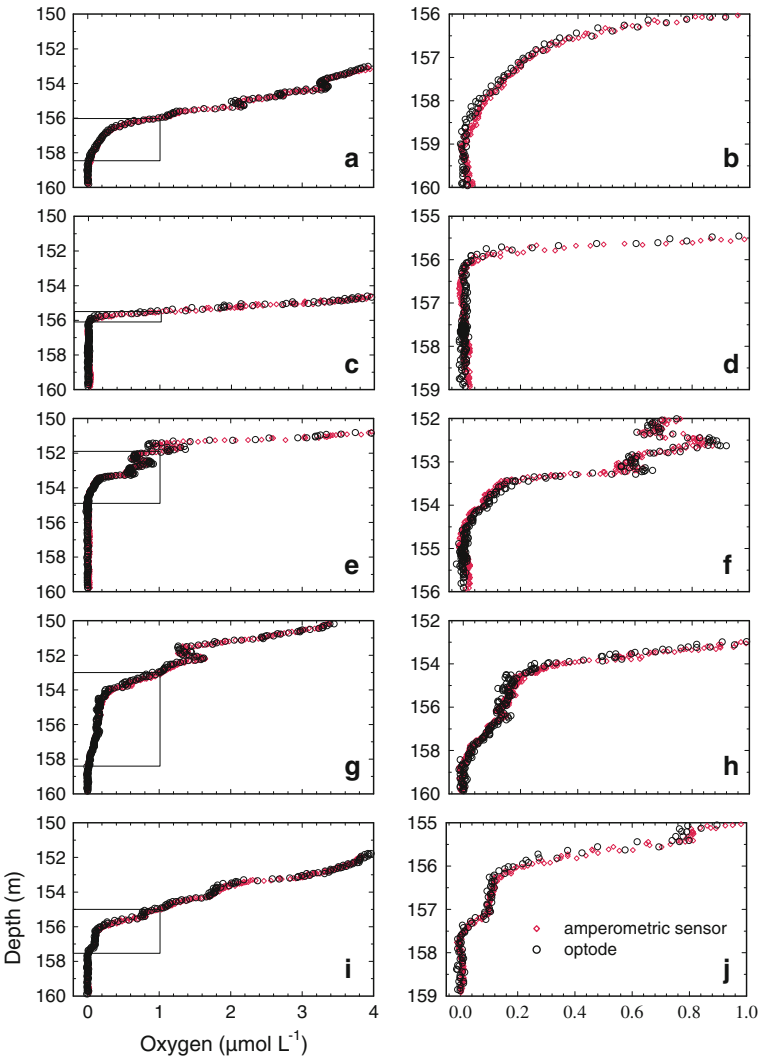

Fig. 5 Lake Zug, August 7, 2010: High-resolution oxygen profiles across the oxic–anoxic interface showing the variability of the submicromolar zone. Profiles were measured with two independent systems (amperometric microsensor and microoptode) deployed in parallel with sensor tips separated horizontally by 1 cm. The *rectangles* in the *left panels* indicate the submicromolar zone (1,000–10 nmol O_2 L^{-1}) shown in detail in the *right panels* (note different depth scale in panel **h**). The correlation coefficient between the presented amperometric and optical data is at least 0.995. Further details of the casts are summarized in Table 1

and an evaluation of the anoxic offset between this ex situ calibration and field observations. The maximum deviation of < 24 nmol L^{-1} was small and indicates that the microoptode performance at low oxygen levels is nearly unaffected by previous exposure to high oxygen concentrations. The amperometric system was then calibrated based on the microoptode. Thus, the good correspondence of the amperometric results with CTD-derived oxygen concentrations > 200 µmol L^{-1} corroborates the valid calibration of both systems.

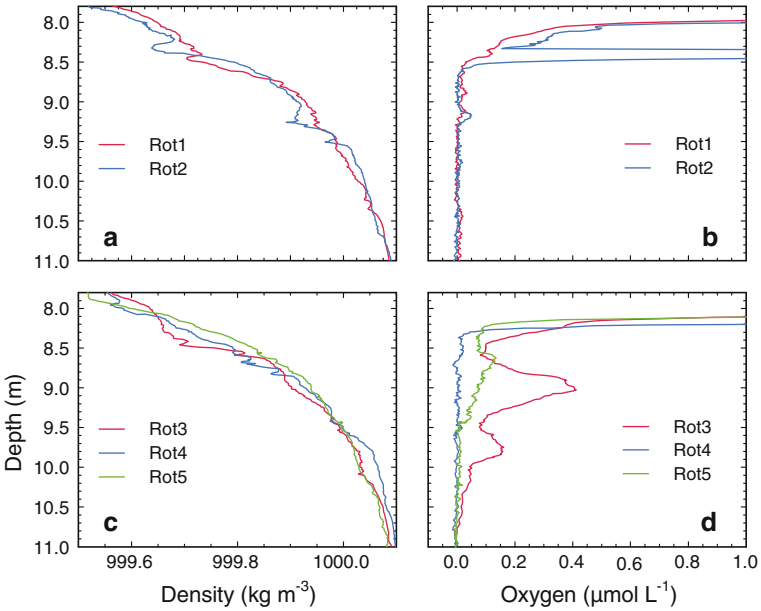

Fig. 6 Lake Rot, October 19, 2010: Density profiles (**a**, **c**) and high-resolution oxygen profiles measured with the microoptode (**b**, **d**) across the lower end of the oxycline. Further details of the casts are summarized in Table 1

3.3 Microoptode Profiles Across a Temperature Gradient

The microoptode's applicability across an anoxic temperature gradient was investigated in Lake Rot. The deep lakes Lugano and Zug had negligible temperature gradients across the redoxcline, but at the metalimnion in Lake Rot, the temperature changed by up to -2.7 °C m^{-1} on the October 19, 2010 (Fig. 3c).

The temperature dependence of the fluorescence lifetime caused a change in the phase angle in anoxic waters of -0.09 ± 0.02 °C^{-1} ($n = 4$) which corresponded to an uncorrected in situ oxygen decrease of $\sim 26.7 \pm 4.7$ nmol L^{-1} °C^{-1} ($n = 4$). After temperature compensation, this change was reduced to $\sim 5.8 \pm 2.1$ nmol L^{-1} °C^{-1} ($n = 4$). Thus, already the manufacturer-provided algorithm compensated the microoptode's temperature dependency to an acceptable limit and provided close to constant anoxic profiles (Fig. 6b, c). For the campaign in Lake Rot, the in situ detection limit of the applied microoptode was 9.6 ± 0.3 nmol O_2 L^{-1} ($n = 4$).

3.4 Submicromolar Zones in a Deep Hypolimnion

To avoid the conceptually ill-defined term "suboxic zone" (Canfield and Thamdrup 2009), we propose to define the lower end of the oxic zone based on sensitive sensor measurements. In this sense, the submicromolar zone starts below 1 µmol L^{-1} and ends with the typical detection limit of 10 nmol O_2 L^{-1}. In Lake Zug, the thickness of the submicromolar zone in the hypolimnion between 150 and 160 m water depth was evaluated in nine profiles recorded with the dual sensor system (see five examples in Fig. 5). The observed average thickness was 2.7 ± 1.5 m ($n = 9$) with a maximum extension of 5.6 m

(Table 1). The thickness of this zone would have been significantly underestimated (~0.5 m) if calculated from linearly extrapolated oxygen gradients between 20 and 1 μmol L^{-1}. This exemplifies the importance of high-resolution measurements in the nanomolar range.

The shape of the individual profiles could be classified in two different types. The smooth profiles showed continually decreasing oxygen concentrations (Fig. 5b, d), while other oxic–anoxic transitions were characterized by inversions and O_2 peaks (Fig. 5f, h, j). The position of the oxic–anoxic interface (10 nmol O_2 L^{-1}) varied several meters in depth between the casts (Table 1). However, the oxic–anoxic interfaces were not associated with a specific density-horizon (data not shown), and thus, internal waves cannot explain the variations in oxic/anoxic interface depth.

Submicromolar zones with similar shapes and a varying depth of the oxic–anoxic interface were observed as well in Lake Lugano. The submicromolar zones extended on average over 1.55 ± 0.36 m ($n = 3$) (Table 1), although the linear extrapolation of the large-scale oxygen gradient implied an extension over only ~0.3 m.

3.5 Submicromolar Zones at a Thermocline

The large-scale oxygen gradient in Lake Zug extended over more than 100 m water depth, whereas oxygen in Lake Rot dropped from ~350 μmol L^{-1} in the fully mixed epilimnion (0–7.6 m) to ~1 μmol L^{-1} near 8.1 m due to a strong thermal stratification (Fig. 3c). In spite of these contrasting differences in the physical regime, the observed features of the submicromolar zone in Lake Rot were quite similar to those in Lake Zug (Fig. 6). A linear extrapolation of the O_2 gradient predicted a submicromolar zone in the range of centimeters. However, the submicromolar zone extended on average over 1.0 m ± 1.0 m ($n = 5$), but varied strongly between 0.2 and 2.5 m (Table 1). The depth of the oxic–anoxic interface varied accordingly. Again, the microoptode recorded both types of profiles, smooth transitions of the overall oxygen gradient to the constant anoxic levels and sharp inversions and maxima in submicromolar O_2 concentrations (Fig. 6). However, distinct structures in the density profiles matched only occasionally with inversed oxygen gradients (Fig. 6a, cast Rot2 at 8.4 m), while most density discontinuities have no counterpart in the oxygen profiles (Fig. 6a, c, casts Rot1, Rot3 at 8.4 m).

3.6 Governing Factors for Submicromolar O_2 Variability

Our profiling study revealed submicromolar layers of a thickness on the order of a meter within the stable thermocline of Lake Rot and up to several meters in the quasi-homogeneous hypolimnion of Lake Zug. The spatial extension of this transition zone, the considerable variability of the oxygen profiles and the strongly differing depths of the oxic–anoxic interface were unexpected features of this lower boundary of the oxic zone. However, we carefully reduced the risk of sampling artefacts like self-induced turbulent mixing from previous casts by horizontal movement of the probe to an unsampled spot prior to profiling.

Several physical and biogeochemical factors could contribute to the oxygen variability at the oxic–anoxic transition: Vertical (diapycnal) mixing occurs mostly at the boundaries and not in the center of lakes where the profiles were taken. The turbulence in the interior of the hypolimnion is extremely weak, and the energy transfer from large-scale seiching to turbulent mixing occurs in the bottom boundary layer (Wüest and Lorke 2003; Goudsmit et al. 1997). Horizontal mixing in deep lakes is typically 4–5 orders of magnitude more

effective than vertical mixing with tracer fronts moving in the horizontal direction on the order of a kilometer per day (Peeters et al. 1996). As a result, the biogeochemical profiles in the interior of a lake are strongly affected by the intermittent reaction and transport processes occurring at the boundaries (Lorke et al. 2003; Brand et al. 2008; Müller et al. 2012). In addition, slow respiration reactions with half-lives on the order of days rather than hours (Stolper et al. 2010) could further modulate the submicromolar O_2 concentrations close to the oxic–anoxic boundary. The boundary layer mixing could thus not only promote lateral injection of oxygen as observed, e.g., in the Black Sea (Konovalov et al. 2003), but could as well continuously feed different concentrations of microorganisms towards the calm interior of the lake which could further enhance the contrast of biogeochemical conditions of adjacent water parcels. Such a regime is quite plausible for Lake Rot where patchiness in algal activity could modulate the balance of photosynthesis and respiration even down to the oxic–anoxic interface. Further time-series measurements and analyses of the microbial activity at the oxic–anoxic interface will help to discriminate between the governing mechanisms of submicromolar O_2 variability.

4 Final Assessment and Conclusion

In this study, we demonstrate that amperometric microsensors as well as microoptodes, and thus two completely different O_2-sensing systems, allow reliable resolution of the fine-scale structure of the oxic–anoxic interface down to the 10 nmol O_2 L^{-1} range in a continuous profiling mode. The excellent match of the profiles in the submicromolar oxygen range during dual profiling indicates that the observed patterns are caused by actual concentration gradients and not by problems of the sensing system or measuring principle.

The PIA's combination of high-resolution in situ sensing, sampling capability and online data transfer makes the observed extensive submicromolar zones now accessible for detailed studies and provides fast localization of the oxic–anoxic interface which in turn might be used as anchor point for targeted sampling.

Reduction in amperometric signal drift at low to anoxic oxygen concentrations was the key to access the nanomolar range without the need for intermittent internal calibration (Revsbech et al. 2009), thus allowing continuous profiling. The in situ studies demonstrated that anoxic preconditioning of common amperometric microsensors strongly reduced signal drift at low oxygen concentration. The stabilized signal then allowed use of the anoxic part of the water column for zero baseline calibration. Detection limits below 10 nmol L^{-1} were achieved by the employed high amplification scheme which realized high signal resolution (<0.06 nmol L^{-1} bit^{-1}) at low oxygen concentrations. The stable signals and the low detection limits improved the localization of the oxic–anoxic interface clearly (Fig. 4). This amperometric approach provides a continuous signal which can be sampled at the desired temporal resolution which we set at 2 Hz.

The field experiments revealed some limitations for the amperometric system: Stable zero oxygen signals are currently only achieved after 2–4 h of anoxic preconditioning and only in H_2S-free waters (Fig. 4). Low drift can only be maintained by limiting the sensor's exposure to oxygen during profiling. For measurements across a significant temperature gradient, the temperature dependency ($\approx$2–3 % per °C) should be evaluated for each microsensor (Reimers 1987; Gundersen et al. 1998). Furthermore, electromagnetic noise, e.g., as emitted during operation of the syringe sampler, will propagate as strong peaks into the highly amplified amperometric signal which impedes exact measurements during sampling.

While achieving nearly similar detection limits, the microoptode offers therefore several advantages for sampling purposes and in sulfidic waters: The optical principle is insensitive to electromagnetic noise, and drift stability is realized without long preconditioning times. Precise oxygen measurements are recorded even during sampler operation and consecutive transfers through the oxic water column, e.g., to retrieve samples are unproblematic. The small anoxic offsets below 24 nmol L^{-1} thereby corroborated the long-term stability of the calibration. The microoptode's zero oxygen signal is unaffected by free H_2S, and its temperature dependency is well compensated by the manufacturer-supplied algorithm (Fig. 6).

In contrast to the amperometric system, the microoptode's fluorescence intensity and lifetime increase with decreasing oxygen partial pressure which contributes to stable zero oxygen signals. Compared to the amperometric setup, the microoptode had a lower maximal digital resolution of $\sim$4 nmol L^{-1} per 0.01° increment in phase shift. But due to the stable zero oxygen signals, the microoptode's in situ detection limits were still well below 20 nmol L^{-1} and are acceptable for submicromolar profiling. Similar to the amperometric system, the microoptode could provide a nearly continuous signal, but currently the maximum sampling frequency is limited to 1 Hz by its opto-electronics. However, optical systems with faster sampling rates have been described recently (Chipman et al. 2012).

Surface-wave-induced motion of the probe during casts can set a lower limit to acceptable dive speeds for ship-based high-resolution profiling, and thus, fast responding sensing systems are desirable. The 90 %-response times of our amperometric and optical systems were 9 and 7 s, respectively. Faster sensors are available and would further improve the performance in profiling highly variable oxygen regimes: The amperometric system still allows for significant optimization of the response time to $\leq$0.2 s (Chipman et al. 2012; Berg et al. 2003), and a more quantitative design of the back guard cathode might shorten preconditioning times. Similar, fast optodes with signal responses $\leq$0.2 s have been described recently, and new technologies for high sensitivity measurements are emerging (Chipman et al. 2012; Mayr et al. 2009). However, for wavy field sites, a free-falling deployment with slow sinking speeds could be advantageous to achieve high spatial resolution and to precisely locate the oxic–anoxic interface.

The high-resolution profiles obtained by the two methods and with the PIA-system revealed hitherto unnoticed extensive submicromolar zones in lakes with strongly differing vertical stratification. The depth of the oxic–anoxic interface as well as the spatial distribution of submicromolar oxygen concentrations varied between casts, showing highly dynamic systems. The linear extrapolation from micromolar oxygen gradients to zero oxygen underestimated the thickness of the submicromolar zones severalfold and cannot account for the observed small-scale variability. Thus, we cannot assume zero oxygen concentration and "anoxic" conditions at depths directly below the 1 μmol L^{-1} detection limit of conventional O_2 sensors. Therefore, part of the discussion of a "lack of overlap" in gradients of the terminal electron acceptor O_2 and reduced substances such as NH_4^+, H_2S and CH_4 (Murray et al. 1995; Schubert et al. 2010) needs to be refocused on the potential of chemotrophic reactions occurring at submicromolar O_2 concentrations, on the physical transfer of O_2 to the lowest end of the oxic zone, and on the importance of deep oxygenic photosynthesis in shallow aquatic systems. With their broad range of redox conditions, lakes are accessible test systems for such studies. Profiling capabilities beyond the micromolar limit will facilitate the design and execution of further studies on the coupling of carbon and nutrient cycles at these redox boundaries (Wright et al. 2012; Lam and Kuypers 2011; Dellwig et al. 2010).

Acknowledgments For fruitful discussions, we thank Eric Epping, Jan Fischer, Volker Meyer and Hans Røy. We thank Dörte Carstens, Alois Zwyssig and Ruth Stierli for help in the laboratory and in the field. Hans Røy, Alfred Wüest, B. Bohnenbuck, Moritz Holtappels, Jan Fischer, Andreas Brand and Helmut Bürgmann commented on the previous version of the manuscript. The project was funded by Eawag and benefitted from the interaction with team members of the EU-project "HYPOX" (EC Grant # 226213).

References

Balcke GU, Wegener S, Kiesel B, Benndorf D, Schlomann M, Vogt C (2008) Kinetics of chlorobenzene biodegradation under reduced oxygen levels. Biodegradation 19(4):507–518. doi:10.1007/s10532-007-9156-0

Barbieri A, Polli B (1992) Description of Lake Lugano. Aquat Sci 54(3–4):181–183. doi:10.1007/BF00878135

Benson BB, Krause D (1984) The concentration and isotopic fractionation of oxygen dissolved in freshwater and seawater in equilibrium with the atmosphere. Limnol Oceanogr 29(3):620–632. doi:10.4319/lo.1984.29.3.0620

Berg P, Roy H, Janssen F, Meyer V, Jorgensen BB, Huettel M, de Beer D (2003) Oxygen uptake by aquatic sediments measured with a novel non-invasive eddy-correlation technique. Mar Ecol Prog Ser 261:75–83. doi:10.3354/Meps261075

Berner RA (1981) A new geochemical classification of sedimentary environments. J Sediment Petrol 51(2):359–365. doi:10.1306/212F7C7F-2B24-11D7-8648000102C1865D

Brand A, McGinnis DF, Wehrli B, Wüest A (2008) Intermittent oxygen flux from the interior into the bottom boundary of lakes as observed by eddy correlation. Limnol Oceanogr 53(5):1997–2006. doi:10.4319/lo.2008.53.5.1997

Canfield DE, Thamdrup B (2009) Towards a consistent classification scheme for geochemical environments, or, why we wish the term 'suboxic' would go away. Geobiology 7(4):385–392. doi:10.1111/j.1472-4669.2009.00214.x

Chipman L, Huettel M, Berg P, Meyer V, Klimant I, Glud R, Wenzhoefer F (2012) Oxygen optodes as fast sensors for eddy correlation measurements in aquatic systems. Limnol Oceanogr Methods 10:304–316. doi:10.4319/lom.2012.10.304

Clark LC, Wolf R, Granger D, Taylor Z (1953) Continuous recording of blood oxygen tensions by polarography. J Appl Physiol 6(3):189–193

Cline JD (1969) Spectrophotometric determination of hydrogen sulfide in natural waters. Limnol Oceanogr 14:454–458

Dellwig O, Leipe T, Marz C, Glockzin M, Pollehne F, Schnetger B, Yakushev EV, Bottcher ME, Brumsack HJ (2010) A new particulate Mn–Fe–P-shuttle at the redoxcline of anoxic basins. Geochim Cosmochim Acta 74(24):7100–7115. doi:10.1016/j.gca.2010.09.017

Garcia HE, Gordon LI (1992) Oxygen solubility in seawater—better fitting equations. Limnol Oceanogr 37(6):1307–1312. doi:10.4319/lo.1992.37.6.1307

Goudsmit GH, Peeters F, Gloor M, Wüest A (1997) Boundary versus internal diapycnal mixing in stratified natural waters. J Geophys Res Oceans 102(C13):27903–27914. doi:10.1029/97JC01861

Gundersen JK, Ramsing NB, Glud RN (1998) Predicting the signal of O_2 microsensors from physical dimensions, temperature, salinity, and O_2 concentration. Limnol Oceanogr 43(8):1932–1937

Hofmann AF, Peltzer ET, Walz PM, Brewer PG (2011) Hypoxia by degrees: establishing definitions for a changing ocean. Deep Sea Res Part I 58(12):1212–1226. doi:10.1016/j.dsr.2011.09.004

Holst GA, Kuehl M, Klimant I (1995) Novel measuring system for oxygen micro-optodes based on a phase modulation technique. Proc SPIE 2508:387–398. doi:10.1117/12.221754

Holst G, Klimant I, Kühl M, Kohls O (2000) Optical microsensors and microprobes. In: Varney MS (ed) Chemical sensors in oceanography, vol 1. Gordon and Breach Science Publishers, London

Imboden DM, Wüest A (1995) Physics and chemistry of lakes, 2nd edn. Springer, Berlin

Kalvelage T, Jensen MM, Contreras S, Revsbech NP, Lam P, Gunter M, LaRoche J, Lavik G, Kuypers MMM et al (2011) Oxygen sensitivity of anammox and coupled N-cycle processes in oxygen minimum zones. Plos One 6(12). doi:10.1371/journal.pone.0029299

Klimant I, Meyer V, Kuhl M (1995) Fiber-optic oxygen microsensors, a new tool in aquatic biology. Limnol Oceanogr 40(6):1159–1165. doi:0.4319/lo.1995.40.6.1159

Kohler HP, Ahring B, Albella C (1984) Bacteriological studies on the sulfur cycle in the anaerobic part of the hypolimnion and in the surface sediments of Rotsee in Switzerland. FEMS Microbiol Lett 21(3):279–286. doi:10.1111/j.1574-6968.1984.tb00322.x

Konovalov SK, Luther GW, Friederich GE, Nuzzio DB, Tebo BM, Murray JW, Oguz T, Glazer B, Trouwborst RE, Clement B, Murray KJ, Romanov AS (2003) Lateral injection of oxygen with the Bosporus plume—fingers of oxidizing potential in the Black Sea. Limnol Oceanogr 48(6):2369–2376

Lam P, Kuypers MMM (2011) Microbial nitrogen cycling processes in oxygen minimum zones. Annu Rev Mar Sci 3:317–345. doi:10.1146/annurev-marine-120709-142814

Lam P, Lavik G, Jensen MM, van de Vossenberg J, Schmid M, Woebken D, Dimitri G, Amann R, Jetten MSM, Kuypers MMM (2009) Revising the nitrogen cycle in the Peruvian oxygen minimum zone. Proc Natl Acad Sci USA 106(12):4752–4757. doi:10.1073/pnas.0812444106

Lippitsch ME, Pusterhofer J, Leiner MJP, Wolfbeis OS (1988) Fibre-optic oxygen sensor with the fluorescence decay time as the information carrier. Anal Chim Acta 205(1–2):1–6. doi:10.1016/S0003-2670(00)82310-7

Lopes F, Viollier E, Thiam A, Michard G, Abril G, Groleau A, Prevot F, Carrias JF, Alberic P, Jezequel D (2011) Biogeochemical modelling of anaerobic vs. aerobic methane oxidation in a meromictic crater lake (Lake Pavin, France). Appl Geochem 26(12):1919–1932. doi:10.1016/j.apgeochem.2011.06.021

Lorke A, Müller B, Maerki M, Wüest A (2003) Breathing sediments: the control of diffusive transport across the sediment-water interface by periodic boundary-layer turbulence. Limnol Oceanogr 48(6):2077–2085. doi:10.4319/lo.2003.48.6.2077

Maerki M, Müller B, Dinkel C, Wehrli B (2009) Mineralization pathways in lake sediments with different oxygen and organic carbon supply. Limnol Oceanogr 54(2):428–438. doi:10.4319/lo.2009.54.2.0428

Mayr T, Borisov SM, Abel T, Enko B, Waich K, Mistlberger G, Klimant I (2009) Light harvesting as a simple and versatile way to enhance brightness of luminescent sensors. Anal Chem 81(15):6541–6545. doi:10.1021/Ac900662x

Morrison JM, Codispoti LA, Smith SL, Wishner K, Flagg C, Gardner WD, Gaurin S, Naqvi SWA, Manghnani V, Prosperie L, Gundersen JS (1999) The oxygen minimum zone in the Arabian Sea during 1995. Deep Sea Res Part II 46(8–9):1903–1931. doi:10.1016/S0967-0645(99)00048-X

Müller B, Bryant LD, Matzinger A, Wüest A (2012) Hypolimnetic oxygen depletion in eutrophic lakes. Environ Sci Technol 46(18):9964–9971. doi:10.1021/es301422r

Murray JW, Codispoti LA, Friederich GE et al (1995) Oxidation-reduction environments—the suboxic zone in the Black Sea. In: Huang CP, O'Melia CR, Morgan JJ (eds) Aquatic chemistry: interfacial and interspecies processes, vol 244. American Chemical Society: Washington, DC, pp 157–176. doi:10.1021/ba-1995-0244.ch007

Nestler H, Kiesel B, Kaschabek SR, Mau M, Schlomann M, Balcke GU (2007) Biodegradation of chlorobenzene under hypoxic and mixed hypoxic-denitrifying conditions. Biodegradation 18(6):755–767. doi:10.1007/s10532-007-9104-z

Peeters F, Wüest A, Piepke G, Imboden DM et al (1996) Horizontal mixing in lakes. J Geophys Res Oceans 101(C8):18361–18375. doi:10.1029/96JC01145

Reimers CE (1987) An in situ microprofiling instrument for measuring interfacial pore water gradients—methods and oxygen profiles from the North Pacific Ocean. Deep Sea Res Part A 34(12):2019–2035. doi:10.1016/0198-0149(87)90096-3

Revsbech NP (1989) An oxygen microsensor with a guard cathode. Limnol Oceanogr 34(2):474–478. doi:10.4319/lo.1989.34.2.0474

Revsbech NP, Jørgensen BB (1986) Microelectrodes: their use in microbial ecology. Adv Microb Ecol 9:293–352

Revsbech NP, Larsen LH, Gundersen J, Dalsgaard T, Ulloa O, Thamdrup B (2009) Determination of ultra-low oxygen concentrations in oxygen minimum zones by the STOX sensor. Limnol Oceanogr Methods 7:371–381. doi:10.4319/lom.2009.7.371

Revsbech NP, Thamdrup B, Dalsgaard T, Canfield DE (2011) Construction of STOX oxygen sensors and their application for determination of O_2 concentrations in oxygen minimum zones. Methods Enzymol 486:325–341. doi:10.1016/B978-0-12-381294-0.00014-6

Schubert CJ, Durisch-Kaiser E, Wehrli B, Thamdrup B, Lam P, Kuypers MMM (2006) Anaerobic ammonium oxidation in a tropical freshwater system (Lake Tanganyika). Environ Microbiol 8(10):1857–1863. doi:10.1111/j.1462-2920.2006.001074.x

Schubert CJ, Lucas FS, Durisch-Kaiser E, Stierli R, Diem T, Scheidegger O, Vazquez F, Müller B (2010) Oxidation and emission of methane in a monomictic lake (Rotsee, Switzerland). Aquat Sci 72(4):455–466. doi:10.1007/s00027-010-0148-5

Stolper DA, Revsbech NP, Canfield DE (2010) Aerobic growth at nanomolar oxygen concentrations. Proc Natl Acad Sci USA 107(44):18755–18760. doi:10.1073/pnas.1013435107

Tengberg A, Hovdenes J, Andersson HJ, Brocandel O, Diaz R, Hebert D, Arnerich T, Huber C, Kortzinger A, Khripounoff A, Rey F, Ronning C, Schimanski J, Sommer S, Stangelmayer A (2006) Evaluation of

a lifetime-based optode to measure oxygen in aquatic systems. Limnol Oceanogr Methods 4:7–17. doi:10.4319/lom.2006.4.7

Thamdrup B, Dalsgaard T, Revsbech NP (2012) Widespread functional anoxia in the oxygen minimum zone of the Eastern South Pacific. Deep Sea Res Part I 65:36–45. doi:10.1016/j.dsr.2012.03.001

Tonolla M, Peduzzi S, Demarta A, Peduzzi R, Hahn D (2004) Phototropic sulfur and sulfate-reducing bacteria in the chemocline of meromictic Lake Cadagno, Switzerland. J Limnol 63(2):161–170. doi:10.4081/jlimnol.2004.161

Ulloa O, Canfield DE, DeLong EF, Letelier RM, Stewart FJ (2012) Microbial oceanography of anoxic oxygen minimum zones. Proc Natl Acad Sci USA 109(40):15996–16003. doi:10.1073/pnas.1205009109

Winkler LW (1888) Die Bestimmung des im Wasser gelösten Sauerstoffes. Ber Dtsch Chem Ges 21(2):2843–2854. doi:10.1002/cber.188802102122

Wright JJ, Konwar KM, Hallam SJ (2012) Microbial ecology of expanding oxygen minimum zones. Nat Rev Microbiol 10(6):381–394. doi:10.1038/Nrmicro2778

Wüest A, Lorke A (2003) Small-scale hydrodynamics in lakes. Annu Rev Fluid Mech 35:373–412. doi:10.1146/annurev.fluid.35.101101.161220